Scientia Iranica B (2013) 20 (2), 313–321

Sharif University of Technology

Scientia Iranica

Transactions B: Mechanical Engineering

www.sciencedirect.com

Boundary layer flow of an Eyring–Powell model fluid due to a stretching cylinder with variable viscosity

M.Y. Malik *, **A. Hussain**, **S. Nadeem**

Department of Mathematics, Quaid-i-Azam University 45320, Islamabad 44000, Pakistan

Received 24 December 2011; revised 15 December 2012; accepted 15 February 2013

KEYWORDS

Variable viscosity;
Analytical solution;
Eyring–Powell model fluid.

Abstract The present investigation consists of an analytical treatment of a steady boundary layer flow of an Eyring–Powell model fluid due to a stretching cylinder with temperature dependent variable viscosity. The heat transfer analysis is also taken into account. Using usual similarity transformations the governing equations have been transformed into non-linear ordinary differential equations and are solved by a powerful technique; the homotopy analysis method. Two models of variable viscosity, namely, Reynolds' and Vogel's are considered. The convergence is carefully checked by plotting h-curves. The emerging parameters intrinsic to the problem are discussed through graphs.

1. Introduction

Viscosity is physical property of fluids. It is the ratio of shear stress to the shear strain. A large number of papers have been discussed in which fluid viscosity is considered to be constant. However, in nature, we find a very few examples of fluids possessing this property. In certain situations, it is not necessary that the fluid viscosity is constant. It may vary with distance, temperature or pressure. For example in coal slurries the viscosity of the fluid varies with temperature. In general the coefficients of viscosity for real fluids are functions of temperature. In many thermal transport processes, the temperature distribution with in the flow field is not uniform, i.e., the fluid viscosity may be changed noticeably if large temperature differences exist in the system. Therefore, it is highly desirable to take into account the temperature dependent viscosity in momentum as well as in the energy equation. Fluids which do not obey Newton's law of viscosity are known as non-Newtonian fluids. Massoudi and Christie [1] have studied the effects of variable viscosity and viscous dissipation on the flow of a third grade fluid in a uniform pipe. They found the numerical solutions with the help of the straight forward finite difference method. They also discussed that the flow of a fluid-solid mixture is very complicated and may depend on many variables such as physical properties of each phase, size and shape of solid particles. Later on, the influence of constant and space dependent viscosity on the flow of a third grade fluid in a pipe has been discussed analytically by Hayat et al. [2]. The approximate and analytical solutions of non-Newtonian fluid with variable viscosity have been analyzed by Yursoy and Pakdemirili [3] and Pakdemirili and Yilbas [4]. The pipe flow of non-Newtonian fluid with variable viscosity keeping no slip and partial slip has been discussed analytically by Nadeem and Ali [5] and Nadeem et al. [6]. More recently, Nadeem and Akbar [7] studied the effects of temperature dependent viscosity on the peristaltic flow of a Jeffrey-six constant fluid in a uniform vertical tube. Keeping this in mind, we are considering temperature dependent viscosity in our study. Stretching is another important phenomena. A Newtonian fluid flow over a linear stretching surface was first studied by Crane [8]. Various aspects of the flow for stretching surfaces have been discussed in many investigations [9–17]. Wang [18] considered the steady flow of a viscous and incompressible fluid outside a stretching hollow cylinder in ambient fluid at rest. Motivation from above mentioned works leads us to consider a steady boundary layer flow of an Eyring–Powell model fluid due to a stretching cylinder with temperature dependent variable viscosity. The highly non-linear problem is transformed into ordinary differential equations with the help of usual similarity transformations. Reynolds' and Vogel's models of temperature

* Corresponding author. Tel.: +92 5190642182; fax: +92 512275341.
E-mail address: drmymalik@hotmail.com (M.Y. Malik).

Peer review under responsibility of Sharif University of Technology.

Production and hosting by Elsevier

1026-3098 © 2013 Sharif University of Technology. Production and hosting by Elsevier B.V. Open access under CC BY license.
doi:10.1016/j.scient.2013.02.028

dependent viscosity are considered. The analytical solution is obtained using a powerful technique; the homotopy analysis method [19–25]. At the end, the physical behavior of various parameters is depicted through graphs.

2. Mathematical model

For an incompressible fluid the balance of mass and momentum are given by:

$$\begin{aligned} &\operatorname{div}\bar{V} = 0,\\ &\rho\frac{d\bar{V}}{dt} = -\nabla\bar{P} + \operatorname{div}\bar{S}, \end{aligned} \tag{1}$$

where ρ is the density, $\bar{V}$ is the velocity vector, $\bar{P}$ is the pressure $\bar{S}$ is the Cauchy stress tensor, and d/dt represents the material time derivative. The constitutive equation for the Eyring–Powell fluid model is given by [26]:

$$\bar{S} = \mu\nabla\bar{V} + \frac{1}{\beta}\sinh^{-1}\left(\frac{1}{c_1}\nabla\bar{V}\right). \tag{2}$$

and

$$\begin{aligned} &\sinh^{-1}\left(\frac{1}{c_1}\nabla\bar{V}\right) \approx \frac{1}{c_1}\nabla\bar{V} - \frac{1}{6}\left(\frac{1}{c_1}\nabla\bar{V}\right)^3,\\ &\left|\frac{1}{c_1}\nabla\bar{V}\right| \ll 1 \end{aligned} \tag{2a}$$

where μ is the coefficient of shear viscosity, and β and c_1 are the material constants of the Eyring–Powell fluid model.

2.1. description of the problem

Consider the steady flow of an incompressible Eyring–Powell model fluid flow caused by a stretching tube of radius "a" on the axial direction, where z is the axis along the tube length and r is the axis in the radial direction. The surface of the tube is at temperature T_w and the ambient fluid temperature is T_1, where $T_w > T_1$. The governing equations are:

$$\frac{\partial(rw)}{\partial z} + \frac{\partial(ru)}{\partial r} = 0, \tag{1}$$

$$\begin{aligned}
&\rho\left(u\frac{\partial u}{\partial r} + w\frac{\partial u}{\partial z}\right) = \frac{2u}{r}\frac{\partial u}{\partial r} + \frac{2}{r\beta c_1}\frac{\partial u}{\partial r}\\
&\quad - \frac{1}{6r\beta c_1^3}\left\{8\left(\frac{\partial u}{\partial r}\right)^3 + 4\frac{\partial u}{\partial r}\left(\frac{\partial u}{\partial z} + \frac{\partial w}{\partial r}\right)^2\right.\\
&\quad \left. + 2\frac{\partial w}{\partial z}\left(\frac{\partial u}{\partial z} + \frac{\partial w}{\partial r}\right)^2\right\} + 2\mu\frac{\partial^2 u}{\partial r^2} + \frac{2}{\beta c_1}\frac{\partial^2 u}{\partial r^2}\\
&\quad - \frac{4}{\beta c_1^3}\left(\frac{\partial u}{\partial r}\right)^2\frac{\partial^2 u}{\partial r^2} - \frac{1}{3\beta c_1^3}\frac{\partial^2 u}{\partial r^2}\left(\frac{\partial u}{\partial z} + \frac{\partial w}{\partial r}\right)^2\\
&\quad - \frac{1}{3\beta c_1^3}\frac{\partial u}{\partial r}\left(\frac{\partial u}{\partial z} + \frac{\partial w}{\partial r}\right)\left(\frac{\partial^2 u}{\partial r\partial z} + \frac{\partial^2 w}{\partial r^2}\right)\\
&\quad - \frac{2}{3\beta c_1^3}\frac{\partial^2 u}{\partial r^2}\left(\frac{\partial u}{\partial z} + \frac{\partial w}{\partial r}\right)^2\\
&\quad - \frac{4}{3\beta c_1^3}\frac{\partial u}{\partial r}\left(\frac{\partial u}{\partial z} + \frac{\partial w}{\partial r}\right)\left(\frac{\partial^2 u}{\partial r\partial z} + \frac{\partial^2 w}{\partial r^2}\right)\\
&\quad + 2\frac{\partial^2 w}{\partial r\partial z}\left(\frac{\partial u}{\partial z} + \frac{\partial w}{\partial r}\right)^2\\
&\quad + 4\frac{\partial w}{\partial z}\left(\frac{\partial u}{\partial z} + \frac{\partial w}{\partial r}\right)\left(\frac{\partial^2 u}{\partial r\partial z} + \frac{\partial^2 w}{\partial r^2}\right)\\
&\quad + \frac{2\mu u}{r^2} + \frac{2u}{\beta c_1 r^2} - \frac{4u^3}{3\beta c_1^3 r^4},
\end{aligned} \tag{2}$$

$$\begin{aligned}
&\rho\left(u\frac{\partial w}{\partial r} + w\frac{\partial w}{\partial z}\right)\\
&= \mu\left(\frac{\partial^2 u}{\partial r\partial z} + \frac{\partial^2 w}{\partial r^2}\right) + \frac{1}{\beta c_1}\left(\frac{\partial^2 u}{\partial r\partial z} + \frac{\partial^2 w}{\partial r^2}\right)\\
&\quad - 2\mu\frac{\partial^2 w}{\partial z^2} + \frac{2}{\beta c_1}\frac{\partial^2 w}{\partial z^2}\\
&\quad + \frac{1}{r}\left[\begin{array}{l}\mu\left(\dfrac{\partial u}{\partial z} + \dfrac{\partial w}{\partial r}\right) + \dfrac{1}{\beta c_1}\left(\dfrac{\partial u}{\partial z} + \dfrac{\partial w}{\partial r}\right)\\ -\dfrac{1}{6r\beta c_1^3}\left\{\begin{array}{l}4\left(\dfrac{\partial u}{\partial r}\right)^2\left(\dfrac{\partial u}{\partial z} + \dfrac{\partial w}{\partial r}\right)\\ \quad + \left(\dfrac{\partial u}{\partial z} + \dfrac{\partial w}{\partial r}\right)^3\\ +4\dfrac{\partial w}{\partial z}\partial u\partial r\left(\dfrac{\partial u}{\partial z} + \dfrac{\partial w}{\partial r}\right)\\ +4\left(\dfrac{\partial w}{\partial z}\right)^2\left(\dfrac{\partial u}{\partial z} + \dfrac{\partial w}{\partial r}\right)\end{array}\right.\end{array}\right]\\
&\quad - \frac{1}{6r\beta c_1^3}\left\{\begin{array}{l}8\dfrac{\partial u}{\partial r}\dfrac{\partial^2 u}{\partial r^2}\left(\dfrac{\partial u}{\partial z} + \dfrac{\partial w}{\partial r}\right)\\ +4\left(\dfrac{\partial u}{\partial r}\right)^2\left(\dfrac{\partial^2 u}{\partial r\partial z} + \dfrac{\partial^2 w}{\partial r^2}\right)\\ +3\left(\dfrac{\partial u}{\partial z} + \dfrac{\partial w}{\partial r}\right)^2\left(\dfrac{\partial^2 u}{\partial r\partial z} + \dfrac{\partial^2 w}{\partial r^2}\right)\\ +4\dfrac{\partial u}{\partial r}\dfrac{\partial^2 w}{\partial r\partial z}\left(\dfrac{\partial u}{\partial z} + \dfrac{\partial w}{\partial r}\right)\\ +4\dfrac{\partial w}{\partial z}\dfrac{\partial^2 u}{\partial r^2}\left(\dfrac{\partial u}{\partial z} + \dfrac{\partial w}{\partial r}\right)\\ +4\dfrac{\partial w}{\partial z}\dfrac{\partial u}{\partial r}\left(\dfrac{\partial^2 u}{\partial r\partial z} + \dfrac{\partial^2 w}{\partial r^2}\right)\\ +8\dfrac{\partial w}{\partial z}\dfrac{\partial^2 w}{\partial r\partial z}\left(\dfrac{\partial u}{\partial z} + \dfrac{\partial w}{\partial r}\right)\\ +4\left(\dfrac{\partial w}{\partial z}\right)^2\left(\dfrac{\partial^2 u}{\partial r\partial z} + \dfrac{\partial^2 w}{\partial r^2}\right)\end{array}\right\}\\
&\quad - \frac{1}{6r\beta c_1^3}\left\{\begin{array}{l}2\dfrac{\partial^2 u}{\partial z\partial r}\left(\dfrac{\partial u}{\partial z} + \dfrac{\partial w}{\partial r}\right)^2\\ +4\dfrac{\partial^2 w}{\partial z^2}\left(\dfrac{\partial u}{\partial z} + \dfrac{\partial w}{\partial r}\right)^2\\ +4\dfrac{\partial u}{\partial r}\left(\dfrac{\partial u}{\partial z} + \dfrac{\partial w}{\partial r}\right)\left(\dfrac{\partial^2 u}{\partial r\partial z} + \dfrac{\partial^2 w}{\partial r^2}\right)\\ +8\dfrac{\partial w}{\partial z}\left(\dfrac{\partial u}{\partial z} + \dfrac{\partial w}{\partial r}\right)\left(\begin{array}{l}\dfrac{\partial^2 u}{\partial r\partial z} + \dfrac{\partial^2 w}{\partial r^2}\\ +12\left(\dfrac{\partial w}{\partial z}\right)^2\dfrac{\partial^2 w}{\partial z^2}\end{array}\right)\end{array}\right\}
\end{aligned} \tag{3}$$

$$u\frac{\partial T}{\partial r} + w\frac{\partial T}{\partial z} = \alpha\left(\frac{\partial^2 T}{\partial r^2} + \frac{1}{r}\frac{\partial T}{\partial r}\right) \tag{4}$$

subject to the boundary conditions

$$\begin{aligned} &u = 0, \qquad w = w_w, \quad \text{at } r = a\\ &w \to 0, \qquad T \to T_\infty, \quad \text{as } r \to \infty \end{aligned} \tag{5}$$

where u and w are the velocity components along the r and z directions respectively, and $w_w = 2cz$ where c is a constant with positive value. Further α, ν, ρ, T, k and μ are thermal diffusivity, the kinematic viscosity, fluid density, fluid temperature, thermal conductivity and viscosity of the fluid. The dimensionless problem which can describe the boundary flow is given by:

$$\begin{aligned}&\mu \mathrm{Re}\,\eta^2\left(ff''-f'^2\right)+4\left(\mu+M\right)\eta^2 f''+4\left(\mu+M\right)\eta^3 f'''\\&+\frac{16}{3}A\eta^2\left(ff'f'''-\left(f'\right)^2\right)-\frac{8}{3}Af^2f''+16A\eta ff'f''\\&-\frac{304}{3}A\eta^2 ff'f''-\frac{352}{3}A\eta^3 f'(f'')^2+\frac{176}{3}A\eta^2 f''(f')^2\\&+64A\eta f(f'')^2+32A\eta\,(f)^2 f''-32A\eta^3\left(f'\right)^2 f'''\\&+\frac{16}{3}A\eta ff'f'''-16A\eta^2 f\left(f''\right)^2+32A\eta^3 f'f''=0,\end{aligned}\tag{6}$$

$$\eta\theta''+(1+\mathrm{Re}\,\mathrm{Pr}f)\,\theta'=0,\tag{7}$$

where we have used the similarity transformations:

$$\begin{aligned}&\eta=\left(\frac{r}{a}\right)^2,\qquad u=\frac{-caf\,(\eta)}{\sqrt{\eta}},\\&w=2czf'\,(\eta),\qquad \theta\,(\eta)=\frac{T-T_\infty}{T_w-T_\infty}.\end{aligned}\tag{8}$$

Here prime denotes differentiation with respect to η. The dimensionless parameters used are:

$$\begin{aligned}&\mathrm{Re}=\frac{ca^2}{2\nu},\qquad \mathrm{Pr}=\frac{\nu}{\alpha},\\&M=\frac{1}{\mu_*\beta c_1}\qquad A=\frac{c^3}{\mu_*\beta(c_1)^3}.\end{aligned}\tag{9}$$

The boundary conditions in dimensionless form are:

$$\begin{aligned}&f\,(1)=0,\qquad f'\,(1)=0,\qquad \theta\,(1)=1,\\&f'\,(\infty)\to 0,\qquad \theta\,(\infty)\to 0.\end{aligned}\tag{10}$$

3. Series solutions for Reynolds' model

Here, the temperature dependent viscosity is expressed in the form:

$$\mu=e^{-P\theta},\tag{11}$$

which by Maclaurin's series can be written as:

$$\mu=1-P\theta+O(\theta^2).\tag{12}$$

It is worth mentioning that $M=0$ corresponds to the case of constant viscosity. Invoking the above equation into Eqs. (6) and (7) one has:

$$\begin{aligned}&(1-P\theta)\,\mathrm{Re}\,\eta^2\left(ff''-f'^2\right)+4\left((1-P\theta)+M\right)\eta^2 f''\\&+4\left((1-P\theta)+M\right)\eta^3 f'''+\frac{16}{3}A\eta^2\left(ff'f'''-\left(f'\right)^2\right)\\&-\frac{8}{3}Af^2f''+16A\eta ff'f''-\frac{304}{3}A\eta^2 ff'f''-\frac{352}{3}A\eta^3 f'(f'')^2\\&+\frac{176}{3}A\eta^2 f''(f')^2+64A\eta f(f'')^2\\&+32A\eta\,(f)^2 f''-32A\eta^3\left(f'\right)^2 f'''\\&+\frac{16}{3}A\eta ff'f'''-16A\eta^2 f\left(f''\right)^2+32A\eta^3 f'f''=0,\end{aligned}\tag{13}$$

$$\eta\theta''+(1+\mathrm{Re}\,\mathrm{Pr}f)\,\theta'=0.\tag{14}$$

For the HAM solution, we choose the following initial guesses

$$f\,(0)=1-e^{1-\eta},\tag{14a}$$

$$\theta\,(0)=e^{1-\eta},\tag{14b}$$

and linear operators:

$$\mathcal{L}(f)=f'''+f'',\tag{14c}$$

$$\mathcal{L}(\theta)=\theta''+\theta'.\tag{15}$$

The Zeroth order deformation problem is defined as:

$$(1-q)\mathcal{L}_f[\bar{f}(\eta,\,q)-f_o(\eta)]=q\,\hbar_f\,N_f[\bar{f}(\eta,\,q),\,\bar{\theta}(\eta,\,q)],\tag{16}$$

$$(1-q)\mathcal{L}\theta[\bar{\theta}(\eta,\,q)-\theta_o(\eta)]=q\,\hbar_\theta\,N_\theta[\bar{f}(\eta,\,q),\,\bar{\theta}(\eta,\,q)],\tag{17}$$

$$\bar{f}(\eta,\,q)=0,\qquad \bar{\theta}(\eta,\,q)=1,\qquad \bar{f}'(\eta,\,q)=1,\quad \eta=1,\tag{18}$$

$$\frac{\partial\bar{f}(\eta,\,q)}{\partial\eta}=0,\ \bar{\theta}(\eta,\,q)=0,\quad \eta=\infty,\tag{19}$$

$$\begin{aligned}&N_f[\bar{f}(\eta,\,q),\,\bar{\theta}(\eta,\,q)]\\&=(1-P\theta)\,\mathrm{Re}\,\eta^2\left(ff''-f'^2\right)\\&+4\left((1-P\theta)+M\right)\eta^2 f''\\&+4\left((1-P\theta)+M\right)\eta^3 f'''\\&+\frac{16}{3}A\eta^2\left(ff'f'''-\left(f'\right)^2\right)\\&-\frac{8}{3}Af^2f''+32A\eta ff'f''\\&-\frac{304}{3}A\eta^2 ff'f''-\frac{352}{3}A\eta^3 f'(f'')^2\\&+\frac{176}{3}A\eta^2 f''(f')^2+64A\eta f(f'')^2\\&+32A\eta\,(f)^2 f''-32A\eta^3\left(f'\right)^2 f'''\\&+\frac{16}{3}A\eta ff'f'''-16A\eta^2 f\left(f''\right)^2\\&+32A\eta^3 f'f'',\end{aligned}\tag{20}$$

$$N_\theta[\bar{f}(\eta,\,q),\,\bar{\theta}(\eta,\,q)]=\eta\theta''+(1+\mathrm{Re}\;\mathrm{Pr}f)\,\theta',\tag{21}$$

where $q\epsilon[0,\,1]$ is the embedding parameter and $\hbar_f$ and $\hbar_\theta$ are auxiliary non-zero operators.

The mth order deformation equations are defined as:

$$\mathcal{L}_f[f_m(\eta)-\chi_m f_{m-1}(\eta)]=\hbar_f\,R_f(\eta),\tag{22}$$

$$\mathcal{L}_\theta[\theta_m(\eta)-\chi_m\theta_{m-1}(\eta)]=\hbar_\theta\,R_\theta(\eta),\tag{23}$$

where:

$$\chi_m=\begin{cases}0, & m\le 1,\\ 1, & m>1\end{cases}\tag{24}$$

and

$$\begin{aligned}R_f(\eta)=&\,\mathrm{Re}\,\eta^2\left(\sum_{k=0}^{m-1}f_{m-1-k}f_k''-\sum_{k=0}^{m-1}f_{m-1-k}f_k'\right)\\&-P\sum_{k=0}^{m-1}\sum_{l=0}^{k}f_{m-1-k}f_{k-l}''\theta\\&-P\sum_{k=0}^{m-1}\sum_{l=0}^{k}f'_{m-1-k}f'_{k-l}\theta_l+4\,(1+M)\,\eta^2 f''_{m-1}\end{aligned}$$

$$
\begin{aligned}
&-4P\eta^2\sum_{k=0}^{m-1}f''_{m-1-k}\theta_k+4\,(1+M)\;\eta^3 f'''_{m-1}\\
&-4P\eta^3\sum_{m-1}^{k=0}f'''_{m-1-k}\theta_k+\frac{16}{3}A\eta^2\left(\begin{array}{c}\displaystyle\sum_{k=0}^{m-1}\sum_{l=0}^{k}f_{m-1-k}f'_{k-l}f'''_l\\ \displaystyle-\sum_{k=0}^{m-1}f'_{m-1-k}f'_k\end{array}\right)\\
&-8A\sum_{k=0}^{m-1}\sum_{l=0}^{k}f_{m-1-k}f_{k-l}f''_l+16A\eta\sum_{k=0}^{m-1}\sum_{l=0}^{k}f_{m-1-k}f'_{k-l}f''_l\\
&-\frac{304}{3}A\eta^2\sum_{k=0}^{m-1}\sum_{l=0}^{k}f_{m-1-k}f'_{k-l}f''_l\\
&-\frac{352}{3}A\eta^3\sum_{k=0}^{m-1}\sum_{l=0}^{k}f'_{m-1-k}f''_{k-l}f''_l\\
&+\frac{176}{3}A\eta^2\sum_{k=0}^{m-1}\sum_{l=0}^{k}f''_{m-1-k}f'_{k-l}f'_l+64A\eta\sum_{k=0}^{m-1}\sum_{l=0}^{k}f_{m-1-k}f''_{k-l}f''_l\\
&+32A\eta\sum_{k=0}^{m-1}\sum_{l=0}^{k}f_{m-1-k}f_{k-l}f''_l-32A\eta^3\sum_{k=0}^{m-1}\sum_{l=0}^{k}f'_{m-1-k}f'_{k-l}ff'''_l\\
&+\frac{16}{3}A\eta\sum_{k=0}^{m-1}\sum_{l=0}^{k}f_{m-1-k}f'_{k-l}f'''_l-16A\eta^2\sum_{k=0}^{m-1}\sum_{l=0}^{k}f_{m-1-k}f''_{k-l}f''_l\\
&+32A\eta^3\sum_{k=0}^{m-1}f_{m-1-k}f''_k, \qquad (25)
\end{aligned}
$$

$$R_\theta(\eta)=\eta\theta''_{m-1}+\theta'_{m-1}+\mathrm{Re}\;\mathrm{Pr}\sum_{k=0}^{m-1}f_{m-1-k}\theta'_k. \qquad (26)$$

We now use the symbolic software MATHEMATICA and solve the set of linear differential equations (25) and (26) subject to relevant boundary conditions up to the first few order of approximations. It is found that $f_m(\eta)$ and $\theta_m(\eta)$ can be written as:

$$f_m(\eta)=\sum_{n=0}^{m}\sum_{l=0}^{m}b_{m,\,n}\eta^{3n}e^{(2l+1)-(3n+1)\eta}, \qquad (27)$$

$$\theta_m(\eta)=\sum_{n=1}^{m}\sum_{l=0}^{m}d_{m,n}\eta^{3n}e^{2l+3n\eta},\quad m\geq 0.$$

The solution thus can be defined as:

$$f(\eta)=\lim_{Q\to\infty}\left[\sum_{m=0}^{Q}\left(\sum_{n=0}^{m}\sum_{l=0}^{m}a_{m,n}\eta^{3n}e^{(2l+1)-(3n+1)\eta}\right)\right], \qquad (28)$$

$$\theta(\eta)=\lim_{Q\to\infty}\left[\sum_{m=0}^{Q}\left(\sum_{n=1}^{m}\sum_{l=0}^{m}b_{m,n}\eta^{3n}e^{2l+3n\eta}\right)\right]. \qquad (29)$$

4. Series solutions for Vogel's model

Here

$$\mu=\mu_0\exp\left[\frac{n}{(q+\theta)}-\theta_0\right], \qquad (30)$$

which by Maclaurin's series reduces to:

$$\mu=\frac{L}{S}\left(1-\frac{\theta n}{q^2}\right)\quad\text{where } S=\mu_0\exp\left[\frac{n}{q}-\theta_0\right]. \qquad (31)$$

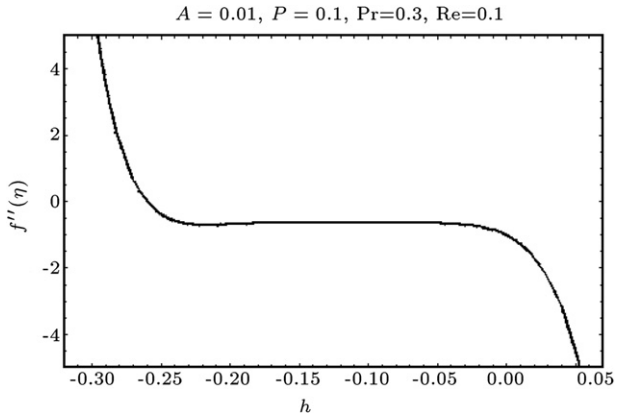

Figure 1: h-curve for velocity profile for Reynolds model.

Invoking the above expression, Eqs. (6) and (7) become:

$$
\begin{aligned}
&\frac{L}{S}\left(1-\frac{\theta n}{q^2}\right)\mathrm{Re}\,\eta^2\left(ff''-f'^2\right)\\
&+4\left(\frac{L}{S}\left(1-\frac{\theta n}{q^2}\right)+M\right)\eta^2 f''\\
&+4\left(\frac{L}{S}\left(1-\frac{\theta n}{q^2}\right)+M\right)\eta^3 f'''+\frac{16}{3}A\eta^2\left(ff'f'''-\left(f'\right)^2\right)\\
&-\frac{8}{3}Af^2f''+32A\eta ff'f''-\frac{306}{3}A\eta^2ff'f''-\frac{352}{3}A\eta^3f'(f'')^2\\
&+\frac{176}{3}A\eta^2f''(f')^2+64A\eta f(f'')^2+32A\eta\,(f)^2f''\\
&-32A\eta^3\left(f'\right)^2f'''+\frac{16}{3}A\eta ff'f'''-16A\eta^2f\left(f''\right)^2\\
&+32A\eta^3f'f''=0, \qquad (32)
\end{aligned}
$$

$$\eta\theta''+(1+\mathrm{Re}\,\mathrm{Pr}f)\,\theta'=0. \qquad (33)$$

Using the similar procedure as discussed in the previous section, the solution of this case is straightforward written as:

$$f_m(\eta)=\sum_{n=0}^{m}\sum_{l=0}^{m}a'_{m,\,n}\eta^{3n}e^{(2l+1)-(3n+1)\,\eta}, \qquad (34)$$

$$\theta_m(\eta)=\sum_{n=1}^{m}\sum_{l=0}^{m}b'_{m,\,n}\eta^{3n}e^{2l-3n\eta},\quad m\geq 0,$$

where $a'_{m,\,n}$ and $b'_{m,\,n}$ are constants.

5. Graphical results and discussion

The governing non-linear partial differential equations of the boundary layer flow and heat transfer of an Eyring–Powell model fluid caused by a stretching tube in the axial direction is presented. First, the governing equations are simplified by using similarity transformation and then the reduced highly nonlinear coupled differential equations are solved analytically with the help of the homotopy analysis method. For the convergence of the HAM solution the h-curves are plotted for velocity and temperature (See Figures 1–4). Figures 1 and 2 correspond to the Reynolds' model which as Figures 3 and 4 relate to Vogel's model. The horizontal lines in these Figures present the convergence region defined by the HAM method.

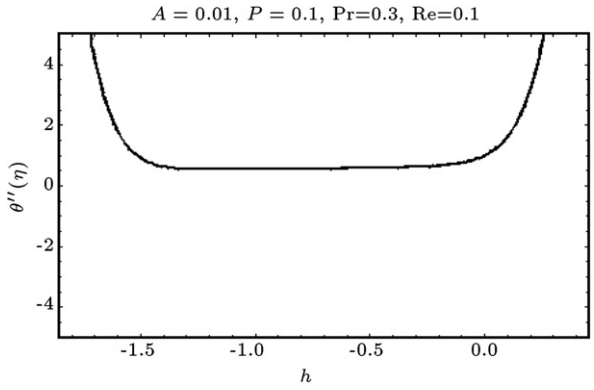

Figure 2: h-curve for temperature profile for Reynolds' model.

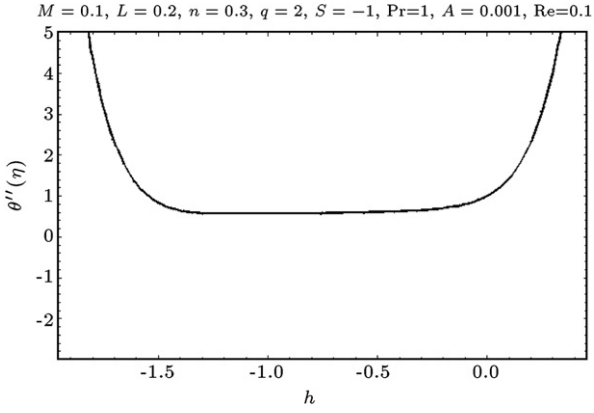

Figure 3: h-curve for temperature profile for Vogel's model.

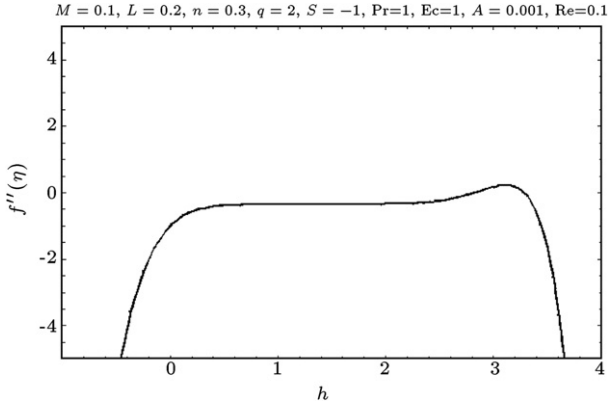

Figure 4: h-curve for velocity profile for Vogel's model.

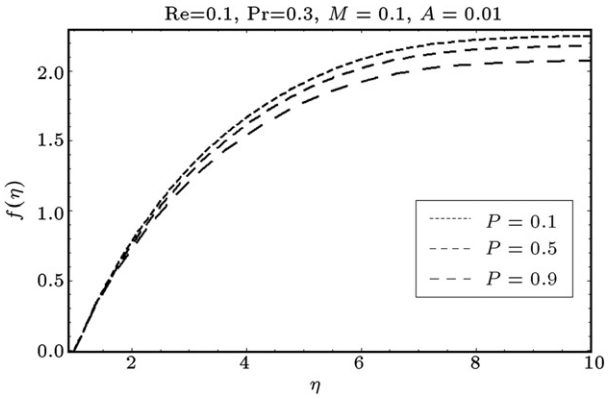

Figure 5: $f(\eta)$ profile for different values of P for Reynolds' model.

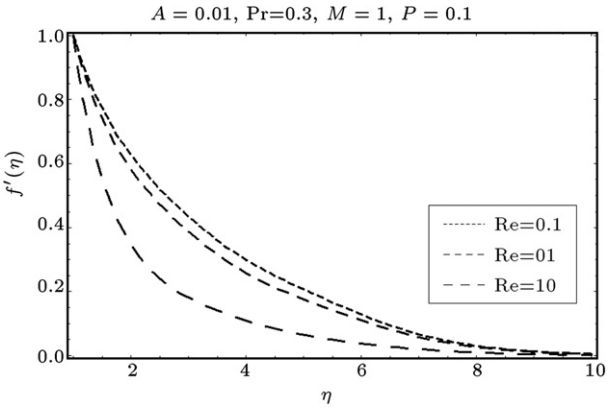

Figure 6: Velocity profile for different values of Re for Reynolds' model.

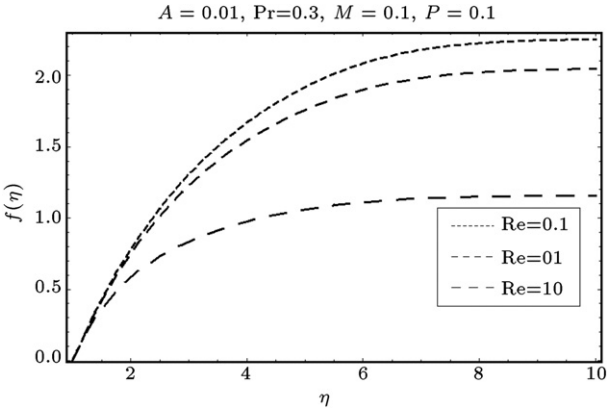

Figure 7: $f(\eta)$ profile for different values of Re for Reynolds' model.

In order to report the effects of sundry parameters in the present investigation we plotted Figures 5–23. Figure 5 shows the $f(\eta)$ profile for different values of P for the Reynolds' model. It is observed that $f(\eta)$ increases from zero. Figure 6 exhibits the velocity profile for different values of Re for the Reynolds' model. It can be seen that velocity decreases as Re increases. Figure 7 shows the $f(\eta)$ profile for the different values of Re for the Reynolds' model. Figure 8 presents velocity profile for different values of A for the Reynolds' model. The velocity profile decreases from 1 to zero as η increases from 1 to ∞. This shows that velocity of the fluid reduces gradually away from the tube surface. Also note that velocity is maximum at the surface of the cylinder. Figure 9 reveals the $f(\eta)$ profile for different values of A for the Reynolds' model. It is concluded that this profile decreases with increase in A. The $f(\eta)$ profile for different values of Pr for the Reynolds' model is displayed in Figure 10. Here, in this case, $f(\eta)$ increases with an increase in Pr. Figure 11 gives the temperature profile for different values

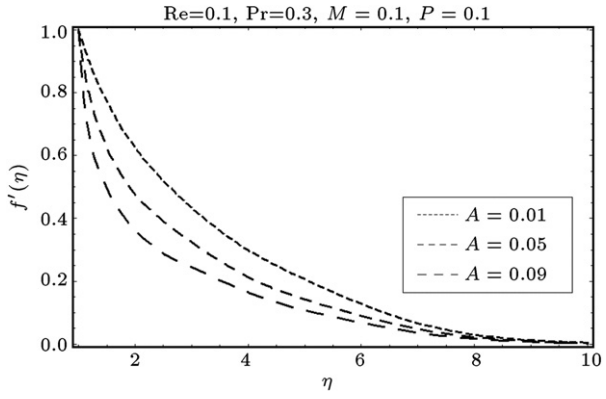

Figure 8: Velocity profile for different values of A for Reynolds' model.

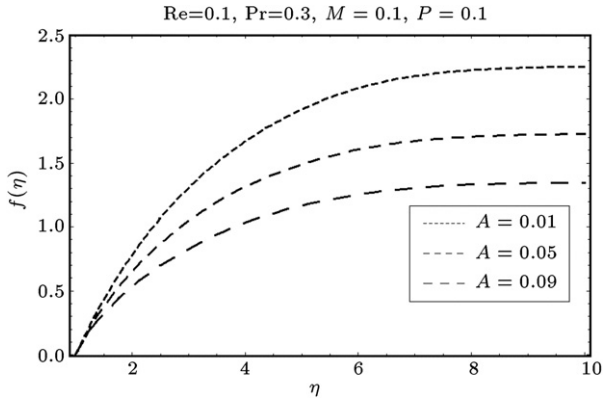

Figure 9: $f(\eta)$ profile for different values of A for Reynolds' model.

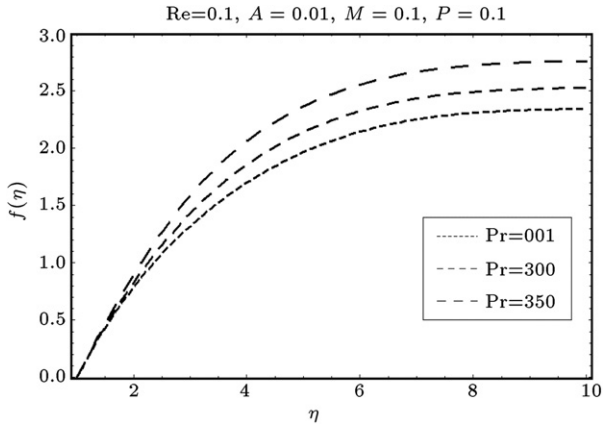

Figure 10: $f(\eta)$ profile for different values of Pr for Reynolds' model.

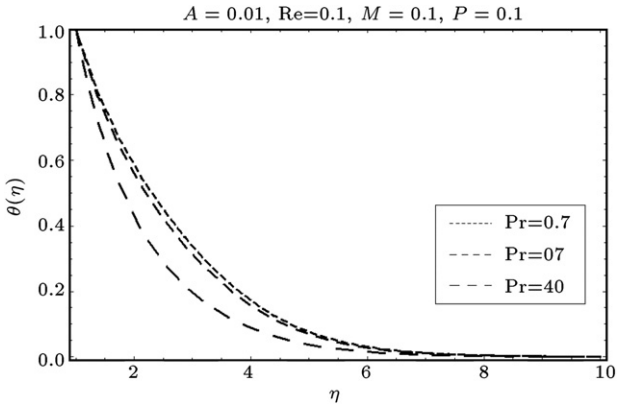

Figure 11: Temperature profile for different values of Pr for Reynolds' model.

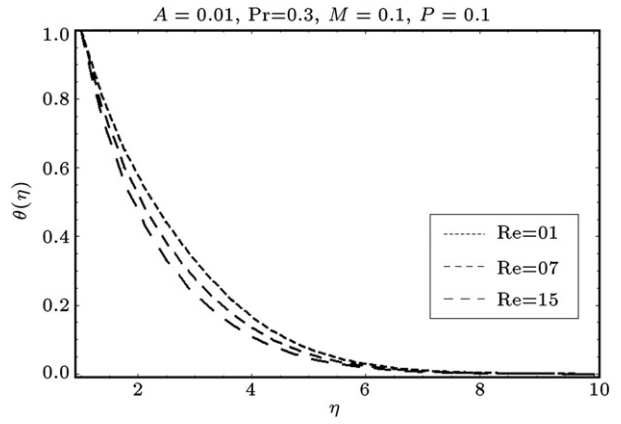

Figure 12: Temperature profile for different values of Re for Reynolds' model.

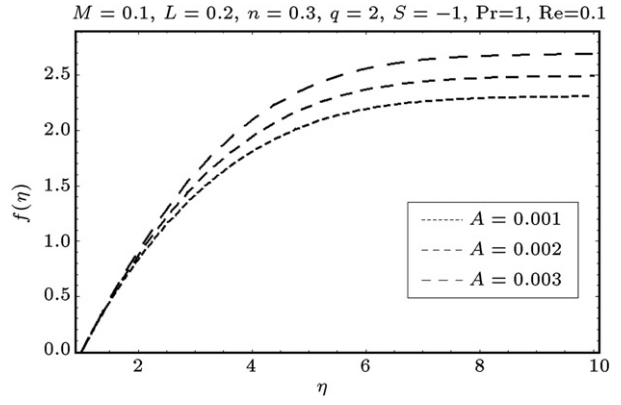

Figure 13: $f(\eta)$ profile for different values of A for Vogel's model.

of Pr for the Reynolds' model. The temperature profiles for air (Pr = .7) and for water (Pr = 7) can be observed here. The temperature profile decreases from 1 to zero as η increases from 1 to ∞. The fluid temperature depends upon the distance from the surface of the tube. The fluid temperature attains maximum value at the surface of the tube. It is noticable that the temperature profile decreases with an increase in Pr. In Figure 12 temperature profile for different values of Re for the Reynolds' model can be seen. Figure 13 exhibits the $f(\eta)$ profile for different values of A for Vogel's model. Figure 14 presents the velocity profile for different values of L for Vogel's model. Figure 15 predicts the $f(\eta)$ profile for different values of M for Vogel's model. Figure 16 is plotted in order to see the $f(\eta)$ profile for different values of n for Vogel's model. Effects of different values of Re on velocity profile for Vogel's model are displayed in Figure 17. Figure 18 shows the $f(\eta)$ profile

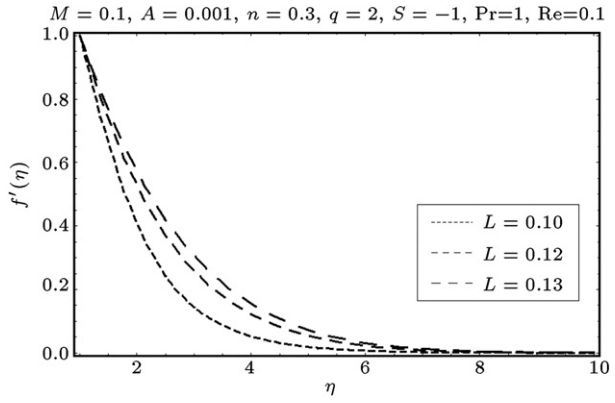

Figure 14: Velocity profile for different values of L for Vogel's model.

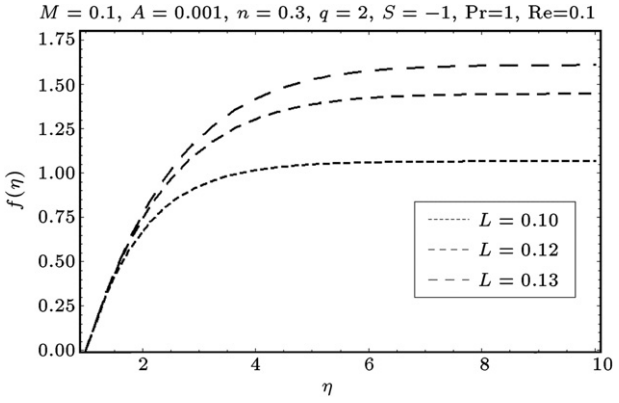

Figure 15: $f(\eta)$ profile for different values of M for Vogel's model.

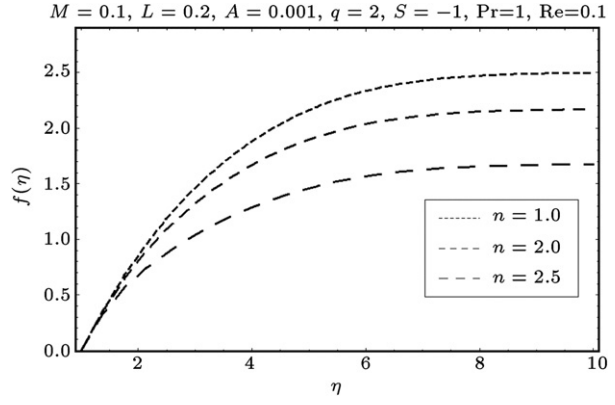

Figure 16: $f(\eta)$ profile for different values of n for Vogel's model.

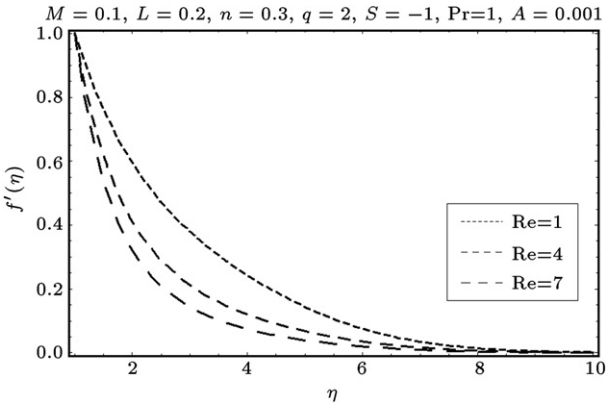

Figure 17: Velocity profile for different values of Re for Vogel's model.

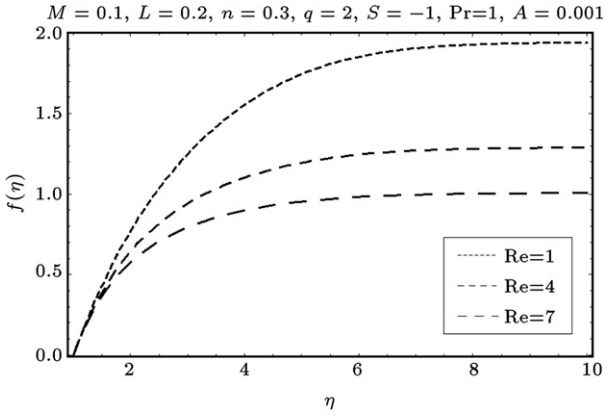

Figure 18: $f(\eta)$ profile for different values of n for Vogel's model.

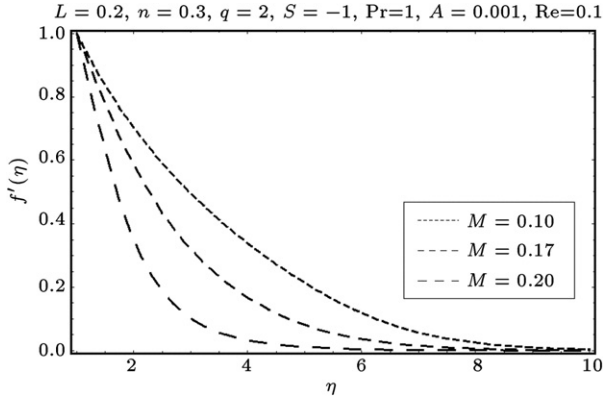

Figure 19: Velocity profile for different values of M for Vogel's model.

for different values of n for Vogel's model. Figure 19 reveals the velocity profile for different values of M for Vogel's model. Figure 20 gives the $f(\eta)$ profile for different values of M for Vogel's model. Temperature profiles for different values of A, Pr and Re for Vogel's model can be observed in Figures 21–23. It is concluded that temperature decreases with an increase in A, Pr and Re. Similar to the case of the Reynolds' model of variable viscosity, the temperature decreases from 1 to zero as the fluid gets away from the outer surface of the cylinder. Maximum temperature is attained at the surface of the tube.

6. Conclusions

In this paper, we have investigated analytically the heat transfer flow of an Eyring–Powell model fluid due to a stretching cylinder. The heat transfer is also taken into account. Two models of variable viscosity, namely, Reynolds' model and Vogel's model are considered. Using usual similarity transformations the governing equations have been transformed

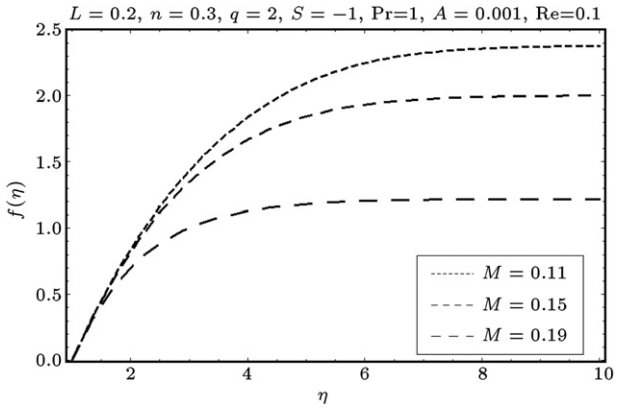

Figure 20: $f(\eta)$ profile for different values of M for Vogel's model.

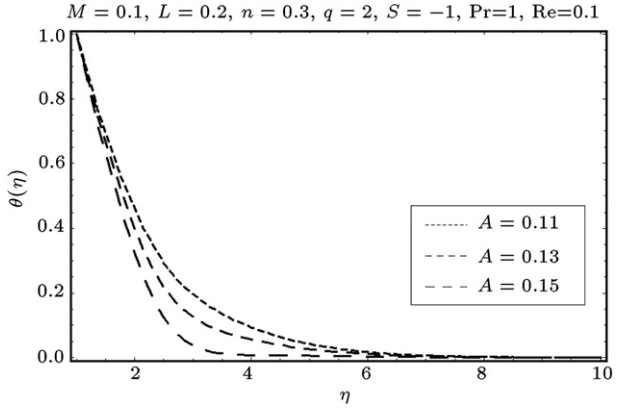

Figure 21: Temperature profile for different values of A for Vogel' model.

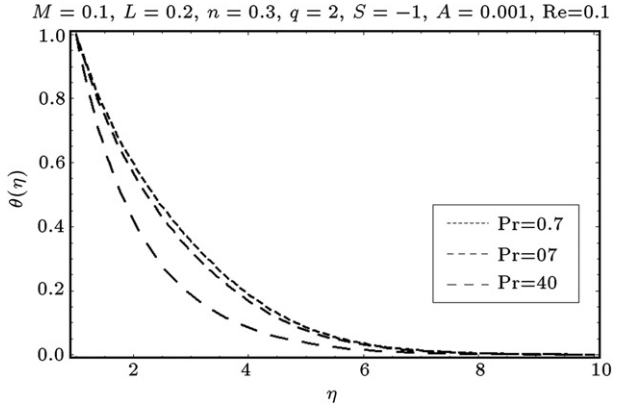

Figure 22: Temperature profile for different values of Pr for Vogel' model.

into non-linear ordinary differential equations. The highly non-linear problem is then solved by the homotopy analysis method. Effects of the various parameters such as Re , A, P, L, n, M and Pr are examined. The velocity and temperature profiles decreases from 1 to zero as η increases from 1 to ∞. The similarity profiles $f(\eta)$ increases from zero, and $f'(\eta)$ decreases from unity. The thermal boundary layer decreases with increased Prandtl number and Reynolds number.

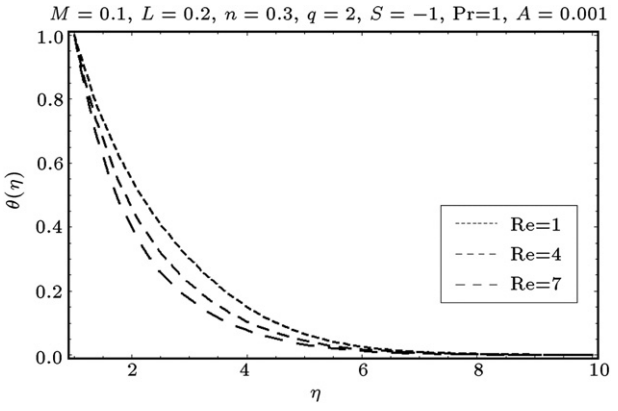

Figure 23: Temperature profile for different values of Re for Vogel's model.

References

[1] Massoudi, M. and Christie, I. "Effect of variable viscosity and viscous dissipation on the flow of a third grade fluid in a pipe", *Int. J. Non-Linear Mech.*, 30, pp. 687–699 (1995).

[2] Hayat, T., Ellahi, R. and Asghar, S. "The influence of variable viscosity and viscous dissipation on the non-Newtonian flow: An analytic solution", *Commun. Nonlinear Sci. Numer. Simul.*, 12, pp. 300–313 (2007).

[3] Yurusoy, M. and Pakdermirli, M. "Approximate analytical solutions for flow of a third grade fluid in a pipe", *Int. J. Non-Linear. Mech.*, 37, pp. 187–195 (2002).

[4] Pakdermirli, M. and Yilbas, B.S. "Entropy generation for pipe flow of a third grade fluid with Vogel model of viscosity", *Int. J. Non-Linear. Mech.*, 41, pp. 432–437 (2006).

[5] Nadeem, S. and Ali, M. "Analytical solutions for pipe flow of a fourth grade fluid with Reynold and Vogel's models of viscosities", *Commun. Nonlinear Sci. Numer. Simul.*, 14, pp. 2070–2090 (2009).

[6] Nadeem, S., Hayat, T., Abbasbandy, S. and Ali, M. "Effects of partial slip on a fourth grade fluid with variable viscosity : An analytical solution", *Nonlinear Anal.: RWA*, 11, pp. 856–868 (2010).

[7] Nadeem, S. and Akbar, N.S. "Effects of temperature dependent viscosity on peristaltic flow of a Jeffrey-six constant fluid in a non-uniform vertical tube", *Commun. Nonlinear Sci. Numer. Simul.*, 15, p. 3950 (2010).

[8] Crane, L.J. "Flow past a stretching plate", *Z. Angew. Math. Phys.*, 21, pp. 645–647 (1970).

[9] Tsou, F.K., Sparrow, E.M. and Goldstein, R.J. "Flow and heat transfer in the boundary layer on a continuous moving surface", *Int. J. Heat Mass Transf.*, 10, pp. 219–235 (1967).

[10] Erickson, L.E., Fan, L.T. and Fox, V.G. "Heat and mass transfer on a moving continuous flat plate with suction or injection", *Ind. Eng. Chem. Fundam.*, 5, pp. 19–25 (1966).

[11] Mucoglu, A. and Chen, T.S. "Mixed convection on inclined surfaces", *ASME J. Heat Transf.*, 101, pp. 422–426 (1979).

[12] Grubka, L.G. and Bobba, K.M. "Heat transfer characteristics of a continuous stretching surface with variable temperature", *ASME J. Heat Transf.*, 107, pp. 248–250 (1985).

[13] Karwe, M.V. and Jaluria, Y. "Fluid flow and mixed convection transport from a moving plate in rolling and extrusion processes", *ASME J. Heat Transf.*, 110, pp. 655–661 (1988).

[14] Chen, C.H. "Laminar mixed convection adjacent to vertical, continuously stretching sheets", *Heat Mass Transf.*, 33, pp. 471–476 (1988).

[15] Abo-Eldahab, E.M. and Abd El-Aziz, M. "Blowing/suction effect on hydromagnetic heat transfer by mixed convection from an inclined continuously stretching surface with internal heat generation/absorption", *Int. J. Therm. Sci.*, 43, pp. 709–719 (2004).

[16] Salem, A.M. and Abd El-Aziz, M. "Effect of Hall currents and chemical reaction on hydromagnetic flow of a stretching vertical surface with internal heat generation/absorption", *Appl. Math. Model.*, 32(7), pp. 1236–1254 (2008).

[17] Abd El-Aziz, M. "Thermal-diffusion and diffusion-thermo effects on combined heat and mass transfer by hydromagnetic three-dimensional free convection over a permeable stretching surface with radiation", *Phys. Lett. A*, 372(4), pp. 263–272 (2007).

[18] Wang, CY. "Fluid flow due to a stretching cylinder", *Phys Fluids*, 31, 466–8 (1988).

[19] Nadeem, S., Hayat, T., Abbasbandy, S. and Ali, M. ''Effects of partial slip on a fourth grade fluid with variable viscosity : An analytical solution'', *Nonlinear Anal.: RWA*, 11, pp. 856–868 (2010).
[20] Ellahi, R. and Afzal, S. ''Effects of variable viscosity in a third grade fluid with porous medium; An analytic solution'', *Commun. Nonlinear Sci. Numer. Simul.*, 14, pp. 2056–2072 (2009).
[21] Malik, M.Y., Hussain, A., Nadeem, S. and Hayat, T. ''Flow of a third grade fluid between coaxial cylinders with variable viscosity'', *Z. Naturforsch.*, 64a, pp. 588–596 (2009).
[22] Nadeem, S. and Akbar, N.S. ''Effects of temperature dependent viscosity on peristaltic flow of a Jeffrey-six constant fluid in a non-uniform vertical tube'', *Commun. Nonlinear Sci. Numer. Simul.*, 15, p. 3950 (2010).
[23] Zedan, Hassan A. and Adrous1, Eman El The Application of the Homotopy Perturbation Method and the Homotopy Analysis Method to the Generalized Zakharov Equations, Abstract and Applied Analysis, http://dx.doi.org/10.1155/2012/561252.
[24] Chaharborj, S.Seddighi, Sadat Kiai, S.M., Abu Bakar, M.R., Ziaeian, I. and Gheisari, Y. ''Homotopy analysis method to study a quadrupole mass filter'', *J. Mass. Spectrom.*, 47, p. 1090 (2012).
[25] Fariborzi Araghia, Mohammad Ali and Fallahzadehb, Amir ''On the Convergence of the Homotopy Analysis Method for Solving the Schrodinger Equation'', *J. Basic. Appl. Sci. Res.*, 2(6), pp. 6076–6083 (2012).
[26] Powell, R.E. and Eyring, H. ''Mechanism for the relaxation theory of viscosity'', *Nature*, 154, pp. 427–428 (1944).

M.Y. Malik's biography was not available at the time of publication.

A. Hussain's biography was not available at the time of publication.

S. Nadeem's biography was not available at the time of publication.